The current issue and full text archive of this journal is available at
www.emeraldinsight.com/0961-5539.htm

Multiple steady state solutions for natural convection in a shallow horizontal rectangular cavity filled with non-Newtonian power-law fluids and heated from all sides

M. Lamsaadi and M. Naïmi
Département de Physique, UFR de Chimie Appliquée et Sciences de l'Environnement, Equipe de Modélisation des Ecoulements et des Transferts, Faculté des Sciences et Techniques, Université Cadi Ayyad, Béni-Mellal, Morocco, and

M. Hasnaoui
Laboratoire de Mécanique des Fluides et d'Energétique, Département de Physique, UFR de Thermique et Mécanique des Fluides, Faculté des Sciences Semlalia, Université Cadi Ayyad, Marrakech, Morocco

Abstract

Purpose – The aim of this work is to study numerically and analytically flow and heat transfer characteristics and multiplicity of steady states for natural convection in a horizontal rectangular cavity, filled with non-Newtonian power-law fluids and heated from all sides.

Design/methodology/approach – The governing equations are discretised by using the well known second-order central finite difference method and integrated by combining the ADI and PSOR techniques. The analytical approach is based on the parallel flow assumption.

Findings – Natural and anti-natural flows existence is proved when the Rayleigh number exceeds a critical value and the side lateral heating intensity values is chosen inside a specific range. The analytical results are found to agree well with those obtained numerically. The fluid flow and the heat transfer are found to be rather sensitive to the non-Newtonian power-law behaviour.

Research limitations/implications – The obtained results are limited to non-Newtonian power-law fluids and cannot be extended to fluids having other behaviours.

Practical implications – The problem is implied in some industrial thermal processes.

Originality/value – Existence of multiple steady state-solutions in the range of the side lateral heating intensity values ensuring, that is reduced by the shear-thickening behaviour and extended by the shear-thinning one for a given value of Rayleigh number.

Keywords Convection, Heat transfer, Numerical analysis, Flow

Paper type Research paper

Nomenclature

A = aspect ratio of the enclosure, equation (10)
a = heat flux ratio
C = dimensionless temperature gradient in x-direction
g = acceleration due to gravity

International Journal of Numerical Methods for Heat & Fluid Flow
Vol. 16 No. 7, 2006
pp. 779-802

0961-5539
DOI 10.1108/09615530610683511

H' = height of the enclosure
k = consistency index for a power-law fluid at the reference temperature
k_0 = parameter of Ellis model, equation (36)
k_1 = parameter of Ellis model, equation (36)
L' = length of the enclosure
m = parameter of Ellis model, equation (36)
n = flow behaviour index for a power-law fluid at the reference temperature
Nu_h = Nusselt number corresponding to the horizontal local heat transfer; equations (11), (12), (31) and (35)
$\overline{Nu}_h$ = Nusselt number corresponding to the horizontal overall heat transfer, equations (13), (31) and (35)
Nu_v = Nusselt number corresponding to the vertical local heat transfer, equations (14) and (32)
$\overline{Nu}_v$ = Nusselt number corresponding to the vertical overall heat transfer, equation (15)
Pr = generalised Prandtl number, equation (10)
q' = constant heat flux per unit area
Ra = generalised Rayleigh number, equation (10)
T = dimensionless temperature, $(T' - T'_c)/\Delta T^*$
T'_c = reference temperature
ΔT^* = characteristic difference of temperature, $q'H'/\lambda$
(u, v) = dimensionless axial and vertical velocities, $(u',v')/(\alpha/H')$
(x, y) = dimensionless axial and vertical coordinates, $(x',y')/H'$

Greek symbols

α = thermal diffusivity at the reference temperature
β = thermal expansion coefficient at the reference temperature
$\dot{\gamma}'_{ij}$ = shear rate tensor
$\dot{\bar{\gamma}}'$ = generalised shear rate
λ = thermal conductivity at the reference temperature
μ = dynamic viscosity for a Newtonian fluid at the reference temperature
μ_a = dimensionless apparent viscosity for a non-Newtonian power-law fluid, equation (6)
Ω = dimensionless vorticity, $\Omega'/(\alpha/H'^2)$
ψ = dimensionless stream function, ψ'/α
ρ = density of fluid at the reference temperature
τ'_{ij} = viscous stress tensor

Superscript

$'$ = dimensional variables

Subscripts

a = threshold value related to the onset of anti-natural flow
c = critical value or value relative to the centre of the enclosure $(x,y) = (A/2,1/2)$
max = maximum value
∞ = asymptotic value

Mathematical symbols

: = dyadic product

Introduction

Many fluids encountered in industrial applications, such as paper making, drilling of petroleum products, slurry transporting, and processing of food and polymers to name a few, exhibit a viscous non-Newtonian behaviour. They have non-linear shear stress – shear rate characteristics that, depending upon their chemistry, can be shear-thinning or shear-thickening. Rheologically, there is a class of purely viscous time-independent fluids that can be modelled by the power-law Ostwald-de Waele constitutive relationship (Bird *et al.*, 1987):

$$\tau'_{ij} = 2\mu'_a \dot{\gamma}'_{ij} = 2k(\dot{\bar{\gamma}}')^{n-1}\dot{\gamma}'_{ij} \tag{1}$$

where it is evident that the apparent viscosity, μ'_a, is a function of the generalised shear rate, $\dot{\bar{\gamma}}' = \sqrt{2\dot{\gamma}'_{ij} : \dot{\gamma}'_{ij}}$. For shear-thinning or pseudo-plastic fluids, the flow behaviour index, n, varies in the range $0 < n < 1$, while for shear-thickening or dilatant ones $n > 1$. In this model, $n = 1$ corresponds to the case of a Newtonian fluid and the

consistency index, k, stands for the dynamic viscosity, μ. Note that the rheological behaviour of many substances can be adequately represented by the Ostwald-de Wale model for relatively large range of shear rates. In addition, this model presents also the advantage of being simple and mathematically tractable compared to the Ellis model since the latter requires at least one more viscosity term, making the determination of the shear stress-shear rate relationship much more difficult.

According to Jaluria (2003), the non-Newtonian fluids are invariably subject to a heat exchange process during either their preparation or transformation to the final product. Then, the thermal processing is often accomplished with the viscous non-Newtonian media and, in some cases, promotes the fluid motion under thermal buoyancy effects inside closed containers. The study conducted by Ozoe and Churchill (1972) counts among the earliest numerical modelling of natural convection in confined non-Newtonian media. The authors determined the threshold of Rayleigh-Bénard convection onset in Ostwald-de Waele power-law fluids. However, their results, related to the critical Rayleigh number, were overestimated experimentally and theoretically by Tien *et al.* (1969) while studying thermal instability of a horizontal layer filled with non-Newtonian power-law fluids and heated from below. After nearly two decades, Turki (1990) investigated numerically a problem of natural convection in a closed rectangular cavity, differentially heated and filled with non-Newtonian fluids. The results obtained were found to be in more or less satisfactory agreement with those obtained experimentally one year before by Cardon (1989). According to Turki's results, the non-Newtonian behaviour may affect considerably the flow structure and heat transfer. More recently, Ohta *et al.* (2002) studied, by a direct numerical analysis, natural convection heat transfer problem of pseudo-plastic fluids confined in a square cavity heated from below and cooled from the top. It was found that the shear-thinning effect leads to an important increase of the heat transfer exchange, and that the locally important change in the viscosity is at the origin of a complicated flow structure observed when the flow behaviour index decreases and the Rayleigh number increases. Afterwards, thermal convection of micro-emulsion slurry, which exhibits a non-Newtonian power-law behaviour, was studied numerically and experimentally by Inaba *et al.* (2003a, b) in rectangular enclosures heated from below and cooled from above with constant but different temperatures. These authors observed that the shear-thinning character leads to an enhancement of the convection heat transfer.

Even though the above studies have considered heating and cooling through two opposite sides while maintaining the remaining other sides insulated, nearly adiabatic conditions are not easy to satisfy in practice. The resulting flow and temperature fields may be quite different from those induced by horizontal or vertical temperature gradients solely. The problem of natural convection in fluid-filled cavities submitted to cross heating was recently studied by Prud'homme and Bougherara (2001) and Prud'homme *et al.* (2003a, b) in tall vertical and shallow horizontal cavities, respectively. A linear stability analysis of the parallel basic flow was used to predict the critical conditions for the development of disturbances.

As the fluid rheology and thermal boundary conditions may play a crucial role in thermal processing, the present work is devoted to study the natural convection heat transfer problem within a two-dimensional horizontal rectangular enclosure filled with a non-Newtonian fluid. The present work was motivated by the fact that the studies dealing with natural convection in closed non-Newtonian fluid-filled

rectangular cavities have received rather sparse attention compared to those related to Newtonian case.

A numerical solution of the full governing equations is obtained for wide ranges of the controlling parameters. In the limit of a shallow cavity, the governing equations can be simplified by using the parallel flow approximation that makes possible their analytical resolution. Fluid flow, temperature fields and heat transfer results are presented for different values of the Rayleigh number, Ra, the power-law index, n, and the constant, a, representing the ratio between the heat flux imposed on the vertical walls and that imposed on the horizontal ones. The competition between the horizontal and vertical imposed heat fluxes is studied and the results presented may be useful to a better understanding of flow and heat transfer characteristics of non-Newtonian fluids submitted to cross gradients of heat.

Problem formulation

A schematic of the studied configuration is shown in Figure 1. The rectangular enclosure, filled with a fluid whose non-Newtonian rheological behaviour is suitable to be described by equation (1), is of height H' and length L' and all its boundaries are rigid, impermeable and subject to constant heat fluxes. The main assumptions made here are those commonly used, i.e. the fluid is incompressible and its physical properties are considered independent of temperature except the density in the buoyancy term which obeys the Boussinesq approximation (Gray and Giorgini, 1976) and the viscous dissipation of fluid is negligible. In addition, it is admitted that the flow is laminar and the third dimension of the cavity is large enough so that the problem can be considered two-dimensional. Then, the dimensionless governing equations, written in terms of vorticity, Ω temperature, T, and stream function, ψ, are the following:

$$\frac{\partial \Omega}{\partial t} + \frac{\partial (u\Omega)}{\partial x} + \frac{\partial (v\Omega)}{\partial y} = Pr\left[\mu_a\left[\frac{\partial^2 \Omega}{\partial x^2} + \frac{\partial^2 \Omega}{\partial y^2}\right] + 2\left[\frac{\partial \mu_a}{\partial x}\,\frac{\partial \Omega}{\partial x} + \frac{\partial \mu_a}{\partial y}\,\frac{\partial \Omega}{\partial y}\right]\right] + S_\Omega \quad (2)$$

$$\frac{\partial T}{\partial t} + \frac{\partial (uT)}{\partial x} + \frac{\partial (vT)}{\partial y} = \frac{\partial^2 T}{\partial x^2} + \frac{\partial^2 T}{\partial y^2} \quad (3)$$

and

$$\frac{\partial^2 \psi}{\partial x^2} + \frac{\partial^2 \psi}{\partial y^2} = -\Omega \quad (4)$$

where

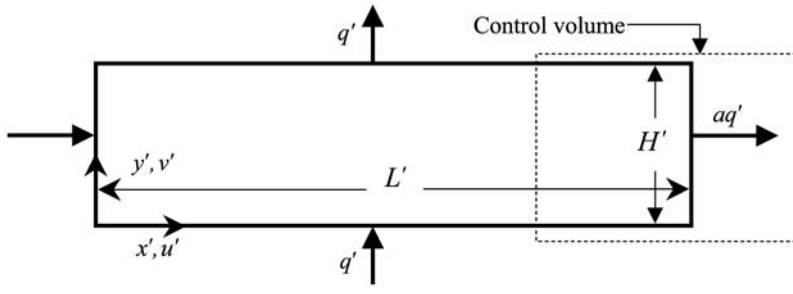

Figure 1.
Sketch of the studied geometry and co-ordinates system

$$u = \frac{\partial \psi}{\partial y}; \; v = -\frac{\partial \psi}{\partial x}, \tag{5}$$

$$\mu_a = \left[2\left[\left(\frac{\partial u}{\partial x}\right)^2 + \left(\frac{\partial v}{\partial y}\right)^2 \right] + \left[\frac{\partial u}{\partial y} + \frac{\partial v}{\partial x}\right]^2 \right]^{\frac{n-1}{2}} \tag{6}$$

and

$$S_\Omega = Pr\left[\left[\frac{\partial^2 \mu_a}{\partial x^2} - \frac{\partial^2 \mu_a}{\partial y^2}\right]\left[\frac{\partial u}{\partial y} + \frac{\partial v}{\partial x}\right] - 2\frac{\partial^2 \mu_a}{\partial x \partial y}\left[\frac{\partial u}{\partial x} - \frac{\partial v}{\partial y}\right] \right] + Pr\, Ra \frac{\partial T}{\partial x} \tag{7}$$

The dimensionless variables are obtained by using the characteristic scales H' H'^2/α, α/H' α/H'^2, $q'H'/\lambda$ and α corresponding to length, time, velocity, vorticity, characteristic temperature and stream function, respectively.

To complete the problem formulation, the following non-dimensional appropriate boundary conditions are used:

$$u = v = \psi = \frac{\partial T}{\partial x} + a = 0 \quad \text{for } x = 0 \quad \text{and } A \tag{8}$$

$$u = v = \psi = \frac{\partial T}{\partial y} + 1 = 0 \quad \text{for } y = 0 \quad \text{and } 1 \tag{9}$$

In addition to the heat flux ratio, a, and the power-law index, n, the present problem is governed by three dimensionless other parameters, namely the aspect ratio of the enclosure, A, the generalised Prandtl number, Pr, and the generalised Rayleigh number, Ra, which are, respectively, defined as follows:

$$A = \frac{L'}{H'}, \quad Pr = \frac{(k/\rho)H'^{2-2n}}{\alpha^{2-n}} \text{ and } Ra = \frac{g\beta H'^{2n+2} q'}{(k/\rho)\alpha^n \lambda} \tag{10}$$

Numerical methodology

The two-dimensional governing equations are solved by using the well-known second order central finite difference method with a regular mesh size. The integration of the vorticity and energy equations (2) and (3), is performed with the alternating-direction implicit method (ADI). This method, frequently used for Newtonian fluids, was successfully extended to non-Newtonian power-law fluids by Ozoe and Churchill (1972), Turki (1990) and Amari *et al.* (1994). To satisfy the conservation of mass, the Poisson equation (equation (3)) was solved by a point successive over-relaxation method (PSOR) with an optimum relaxation factor calculated by the Franckel formula (Roache, 1982). The convergence criterion $\sum_{i,j}|\psi_{i,j}^{k+1} - \psi_{i,j}^{k}| < 10^{-4}\sum_{i,j}|\psi_{i,j}^{k+1}|$ was adopted, where $\psi_{i,j}^{k}$ is the value of the stream function at the kth iteration level. The choice of the mesh grids was based on trial calculations to optimise the computation time and the solutions accuracy. Hence, it is seen from Table I that, for $A = 12$, uniform grids of 241 × 41 are sufficient to model accurately the fluid flow and temperature distribution in the cavity. The time step size was varied from 10^{-6} to 10^{-4} depending on the values of the governing parameters.

Grids		(201 × 41)			(241 × 33)			(241 × 41)			(281 × 41)			(241 × 49)	
n		ψ_{max}	$\overline{Nu_v}$	$\overline{Nu_h}$	ψ_{max}	$\overline{Nu_v}$	$\overline{Nu_h}$	ψ_{max}	$\overline{Nu_v}$	$\overline{Nu_h}$	ψ_{max}	$\overline{Nu_v}$	$\overline{Nu_h}$	ψ_{max}	$\overline{Nu_v}$	$\overline{Nu_h}$
0.6		−10.843	3.534	0.840	−11.869	3.545	0.812	−10.848	3.541	0.839	−10.849	3.541	0.839	−10.828	3.525	0.815
1.0		−3.604	2.549	0.300	−3.595	2.546	0.303	−3.601	2.542	0.301	−3.598	2.537	0.303	−3.600	2.532	0.301
1.4		−1.481	1.507	0.215	−1.471	1.519	0.209	−1.493	1.515	0.217	−1.475	1.496	0.217	−1.466	1.489	0.217

Table I.
Grid size tests conducted for $a = 0.1$, $A = 12$, $Ra = 4,000$ and various values of n (case of natural flow)

Among the various formulae proposed in the literature to evaluate the vorticity on the rigid boundaries, we use here the relation of Woods its accuracy (Roache, 1982).

With the Ostwald power-law model, for $0 < n < 1$, the dimensionless viscosity given by equation (6), tends towards infinity at the immediate vicinity of the corners of the cavity where the velocity gradients are very small which makes impossible direct numerical computations. This numerical difficulty is surpassed by using average values for the corner viscosity which renders the computations possible and stable.

The horizontal local heat transfer through the fluid-filled cavity can be expressed in terms of the local Nusselt number, defined as:

$$Nu_h(y) = \frac{aq'}{(\lambda \Delta T'_h / L')} = \frac{aA}{\Delta T_h} = \frac{a}{(\Delta T_h / A)} \tag{11}$$

where $\Delta T_h = T(0,y) - T(A,y)$ is the side to side horizontal dimensionless local temperature difference. However, this definition is notoriously inaccurate owing to the uncertainty of the temperature values at the two vertical walls due to edge effects. Instead, it is judged preferable to calculate Nu_h on the basis of a difference temperature between two vertical sections, far from the end sides, to improve the accuracy. Thus, by analogy with equation (11), and considering two infinitesimally close sections, Nu_h can be defined by:

$$Nu_h(y) = a \lim_{\delta x \to 0} \frac{\delta x}{\delta T} = a \lim_{\delta x \to 0} \frac{1}{(\delta T / \delta x)} = \frac{-a}{(\partial T / \partial x)_{x=A/2}} \tag{12}$$

where δx is the distance between two symmetrical sections with respect to the central one (section at $x = A/2$). A confirmation of the obviousness of the above remarks is corroborated by the results presented in Table II where the values of the average horizontal Nusselt number are calculated at different locations as follows:

$$\overline{Nu_h} = \int_0^1 Nu_h(y) \mathrm{d}y \tag{13}$$

For the vertical local heat transfer, the following expression is used to evaluate the local Nusselt number:

$$Nu_v(x) = \frac{q'}{(\lambda \Delta T'_v / H')} = \frac{1}{\Delta T_v} \tag{14}$$

where $\Delta T_v = T(x,0) - T(x,1)$ is a vertical dimensionless local temperature difference.

An integration of equation (14) along the horizontal walls leads to the mean vertical Nusselt number:

$$\overline{Nu_v} = \frac{1}{A} \int_0^A Nu_v(x) \mathrm{d}x \tag{15}$$

expressing the vertical overall heat transfer rate across the cavity.

Note that when the flow is parallel, Nu_h and Nu_h, given, respectively, by equations (12) and (14), remain unchanged in the central part of the enclosure.

An additional check of the results accuracy was performed by systematically verifying the energy balance for the system at each numerical code running. Thus, the overall quantity of heat released to the system at $x = 0$ and $y = 0$, was compared to the quantity of heat leaving the latter through the remaining boundaries. For the results reported here, the energy balance was satisfied within 2 per cent as a maximum difference.

Typical streamlines and isotherms, for natural (left) and anti-natural (right) solutions, are shown in Figure 2 for $A = 12$, $Ra = 4{,}000$, $a = 0.1$ and different values of n. In the case of $a = 0$ (absence of side heating), the unicellular flow can rotate either clockwise or counter-clockwise with the same intensity. However, the side heating, as imposed in Figure 1, promotes the clockwise flow and reduces the intensity of the counter-clockwise flow. The terminology "natural" and "anti-natural" is introduced to simply indicate whether the lateral heating is favourable to the flow rotating in one direction "natural" or not "anti-natural". As it can be seen, the flow is parallel to the horizontal boundaries and the temperature is linearly stratified in the horizontal direction for all the considered values of n. The analytical solution, developed in the next section, is based on these observations to allow appropriate simplifications.

Approximate analytical solution

On the basis of the results shown in Figure 2, the following simplifications are used:

$$u(x,y) = u(y), v(x,y) = 0, \quad \psi(x,y) = \psi(y) \quad \text{and} \quad T(x,y) = C(x - A/2) + \theta(y) \tag{16}$$

where C is the unknown but constant dimensionless horizontal temperature gradient in the core region. Using these approximations, the simplified resulting non-dimensional governing equations are:

Table II. Natural flow mean Nusselt number, $\overline{Nu_h}$, calculated at different locations for $a = 0.1$, $A = 12$, $Ra = 4,000$ and various values of n

n	$\delta x = A$	$\delta x = 3A/4$	$\delta x = 2A/3$	$\delta x = A/2$	$\delta x = A/3$	$\delta x \to 0$
			$\overline{Nu_h}$			
0.6	0.770	0.838	0.839	0.839	0.840	0.839
1.0	0.299	0.301	0.301	0.301	0.301	0.301
1.4	0.221	0.216	0.216	0.216	0.217	0.217

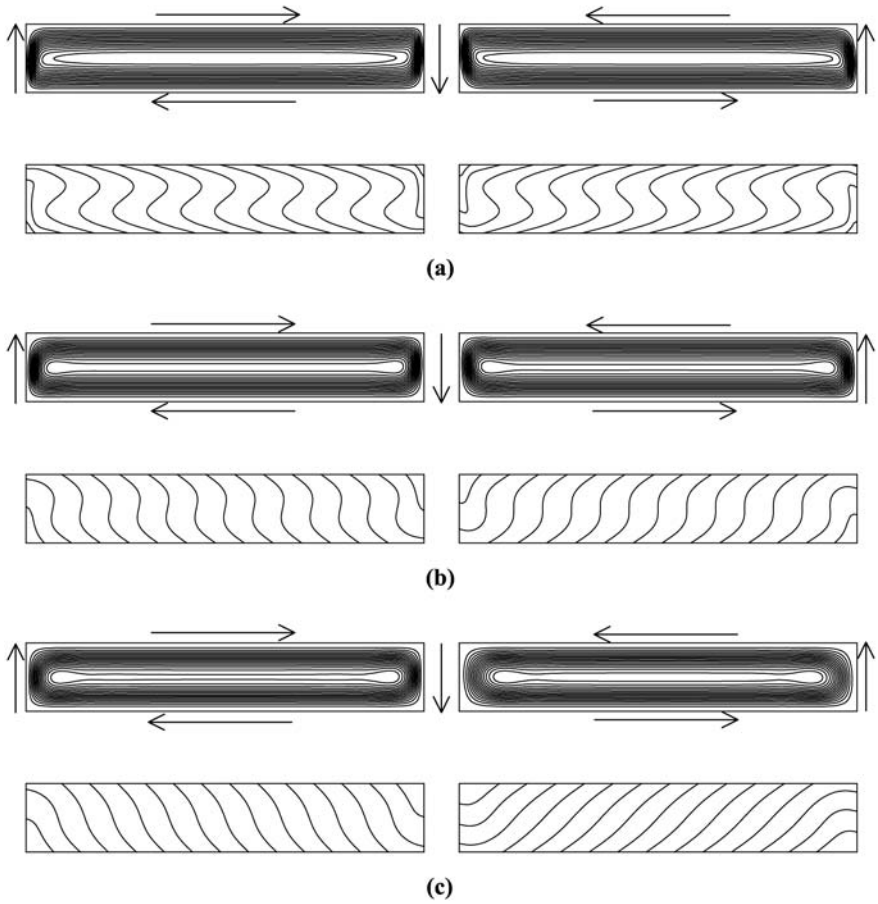

Figure 2.
Natural (left) and anti-natural (right) streamlines (top) and corresponding isotherms (bottom) for $a = 0.1$, $A = 12$, $Ra = 4000$ and various values of n: (a) $n = 0.6$; (b) $n = 1.0$ and (c) $n = 1.4$

$$\frac{\mathrm{d}^2}{\mathrm{d}y^2}\left[\left|\frac{\mathrm{d}u}{\mathrm{d}y}\right|^{n-1}\frac{\mathrm{d}u}{\mathrm{d}y}\right] = CRa \tag{17}$$

$$Cu = \frac{\partial^2 T}{\partial y^2} = \frac{\mathrm{d}^2\theta}{\mathrm{d}y^2} \tag{18}$$

with the following boundary conditions:

$$u = \frac{\mathrm{d}\theta}{\mathrm{d}y} + 1 = 0 \quad \text{for } y = 0 \text{ and } 1 \tag{19}$$

and the return flow condition:

$$\int_0^1 u(y)\mathrm{d}y = 0 \tag{20}$$

In the past, the above concept has been successfully used by many authors in the cases of Newtonian (Sen *et al.*, 1988, Kalla *et al.*, 1999) and non-Newtonian (Amari *et al.*, 1994) fluids.

The integration of equations (17) and (18), associated to the conditions (19) and (20), leads to velocity, temperature and heat transfer rate expressions. Owing to the nature of the governing equations, the operation of integration is complicated and requires a special numerical treatment. Indeed, the non-linearity of the behaviour and the change of the velocity gradient sign due to the return flow, imposes that the velocity expressions are different depending on whether $0 \le y \le y_0$, $y_0 \le y \le y_1$ or $y_1 \le y \le 1$, where y_0 and y_1 ($y_1 = 1 - y_0$, because of the centro-symmetry of the core flow) are the vertical coordinate values for which the vertical velocity gradient is zero. They are derived from equation (20) which is numerically solved by using a combination of the Regula-Falsi and Wegstein iteration methods (Gourdin and Boumahrat, 1989) and the Gauss-Legendre integration method (Sibony and Mardon, 1982). To simplify the velocity and temperature expressions, we introduce the function $f(y) = (y^2 - y + y_0 y_1)/2$. Thus, for $0 \le y \le y_0$, one obtains:

$$u(y) = C^{1/n} Ra^{1/n} \left[\int_0^y \left[f(y) \right]^{1/n} \mathrm{d}y \right] \tag{21}$$

$$\theta(y) = C^{1+1/n} Ra^{1/n} \left[\int_0^y \left[\int_0^y \left[\int_0^y \left[f(y) \right]^{1/n} \mathrm{d}y \right] \mathrm{d}y \right] \mathrm{d}y \right] - y + \theta(0) \tag{22}$$

For $y_0 \le y \le y_1$, the obtained expressions are:

$$u(y) = C^{1/n} Ra^{1/n} \left[\int_0^{y_0} \left[f(y) \right]^{1/n} \mathrm{d}y + \int_y^{y_0} \left[-f(y) \right]^{1/n} \mathrm{d}y \right] \tag{23}$$

$$\begin{aligned} \theta(y) = C^{1+1/n} Ra^{1/n} & \left[\frac{(y - y_0)^2}{2} \int_0^{y_0} \left[f(y) \right]^{1/n} \mathrm{d}y \right. \\ & + \int_{y_0}^{y} \left[\int_{y_0}^{y} \left[\int_{y}^{y_0} \left[-f(y) \right]^{1/n} \mathrm{d}y \right] \mathrm{d}y \right] \mathrm{d}y + (y - y_0) \int_0^{y_0} \left[\int_0^y \left[f(y) \right]^{1/n} \mathrm{d}y \right] \mathrm{d}y \\ & \left. + \int_0^{y_0} \left[\int_0^y \left[\int_0^y \left[f(y) \right]^{1/n} \mathrm{d}y \right] \mathrm{d}y \right] \mathrm{d}y \right] - y + \theta(0) \end{aligned} \tag{24}$$

while for $y_1 \le y \le 1$ the expressions are as follows:

$$u(y) = C^{1/n} Ra^{1/n} \left[\int_0^{y_0} [f(y)]^{1/n} \mathrm{d}y + \int_{y_1}^{y_0} [-f(y)]^{1/n} \mathrm{d}y + \int_{y_1}^{y} [f(y)]^{1/n} \mathrm{d}y \right] \tag{25}$$

$$\begin{aligned}\theta(y)=C^{1+1/n}Ra^{1/n}&\left[\frac{1}{2}(y-y_1)(y+y_1-2)\left[\int_0^{y_0}[f(y)]^{1/n}\mathrm{d}y+\int_{y_1}^{y_0}\left[-f(y)\right]^{1/n}\mathrm{d}y\right]\right.\\&+\int_{y_1}^{y}\left[\int_1^{y}\left[\int_{y_1}^{y}[f(y)]^{1/n}\mathrm{d}y\right]\mathrm{d}y\right]\mathrm{d}y+\int_{y_0}^{y_1}\left[\int_{y_0}^{y}\left[\int_{y}^{y_0}[-f(y)]^{1/n}\mathrm{d}y\right]\mathrm{d}y\right]\mathrm{d}y\\&+\frac{1}{2}(y_1-y_0)^2\int_0^{y_0}[f(y)]^{1/n}\mathrm{d}y+(y_1-y_0)\int_0^{y_0}\left[\int_0^{y}[f(y)]^{1/n}\mathrm{d}y\right]\mathrm{d}y\\&\left.+\int_0^{y_0}\left[\int_0^{y}\left[\int_0^{y}[f(y)]^{1/n}\mathrm{d}y\right]\mathrm{d}y\right]\mathrm{d}y\right]-y+\theta(0)\end{aligned}\tag{26}$$

Taking into account the expressions of $u(y)$ and equation (5), the stream function at the centre of the enclosure can be expressed by:

$$\begin{aligned}\psi_c&=\psi(A/2,1/2)\\&=C^{1/n}Ra^{1/n}\left[(1/2-y_0)\int_0^{y_0}[f(y)]^{1/n}\mathrm{d}y\right.\\&\quad\left.+\int_0^{y_0}\left[\int_0^{y}[f(y)]^{1/n}\mathrm{d}y\right]\mathrm{d}y+\int_{y_0}^{1/2}\left[\int_{y}^{y_0}[-f(y)]^{1/n}\mathrm{d}y\right]\mathrm{d}y\right]\end{aligned}\tag{27}$$

The expression of the constant $\theta(0)$, which is determined by exploiting the centro-symmetry of the core temperature field, is as follows:

$$\begin{aligned}\theta(0)&=1/2-C^{1+1/n}Ra^{1/n}\left[\frac{(1/2-y_0)^2}{2}\int_0^{y_0}[f(y)]^{1/n}\mathrm{d}y\right.\\&\quad+\int_{y_0}^{1/2}\left[\int_{y_0}^{y}\left[\int_{y}^{y_0}[-f(y)]^{1/n}\mathrm{d}y\right]\mathrm{d}y\right]\mathrm{d}y\\&\quad+(1/2-y_0)\int_0^{y_0}\left[\int_0^{y}[f(y)]^{1/n}\mathrm{d}y\right]\mathrm{d}y\\&\quad\left.+\int_0^{y_0}\left[\int_0^{y}\left[\int_0^{y}[f(y)]^{1/n}\mathrm{d}y\right]\mathrm{d}y\right]\mathrm{d}y\right]\\&=1/2-C^{1+1/n}Ra^{1/n}G(n)\end{aligned}\tag{28}$$

On the other hand, the value of the unknown constant C, which characterises the axial temperature gradient, is obtained from the thermal boundary conditions imposed on the end walls. Because of the turning flow at the end regions of the fluid layer, the boundary conditions in the x-direction (equation 8), cannot be exactly satisfied by the parallel flow approximation. According to Bejan (1983), the constant C could be calculated by matching the core solution (equation, 16) to the integral solution for the one of the two end regions (integration of equation (3), together with the boundary conditions (8) and (9), by considering the arbitrary control volume of Figure 1). Taking into account equation (20), this yields the following equation:

$$C + a = \int_0^1 u(y)\theta(y)\mathrm{d}y \tag{29}$$

By substituting the expressions of $u(y)$ and $\theta(y)$ into equation (29), this becomes:

$$C + a = A_n Ra^{2/n} C^{1+2/n} + B_n Ra^{1/n} C^{1/n} \tag{30}$$

The coefficients A_n and B_n, which depend only on n, are calculated by using the Gauss-Legendre integration method and their values are given with those of y_0 in Table III.

To determine the value of C corresponding to given values of n, Ra and a, equation (30) was firstly solved by the Regula-Falsi iteration method and, in order to improve the accuracy, the resulting solution was used as an initial estimation to solve the same equation with the Wegstein iteration method which is of high order than the former.

Using equations (12)-(15) and the centro-symmetrical nature of the solution, the horizontal and vertical Nusselt numbers are constant in the parallel flow region and can be, respectively, expressed as:

$$Nu_{\mathrm{h}} = -\frac{a}{c} = \overline{Nu_{\mathrm{h}}} \tag{31}$$

$$Nu_{\mathrm{v}} = 1/2\theta(0) \tag{32}$$

Two limiting cases are of particular importance:

(1) This case is that of pure conduction regime ($Ra = 0$), for which equations (28) and (30) lead, respectively, to $\theta(0) = 1/2$ and $C = (\partial T/\partial x)_{x=0,A} = -a$. Then, when using equations (31) and (32), one obtains $Nu_{\mathrm{h}} = Nu_{\mathrm{v}} = 1$.

(2) This case corresponds to the limit $\theta(0) \rightarrow 0$ which leads to $Nu_{\mathrm{v}} \rightarrow \infty$ when in equation (28), $C \rightarrow C_\infty$ such us:

$$C_\infty = \frac{1}{[2Ra^{1/n}G(n)]^{n/1+n}} \tag{33}$$

According to equation (30), an asymptotic value of a arises. It is given by:

$$a_\infty = A_n Ra^{2/n} C_\infty^{1+2/n} + B_n Ra^{1/n} C_\infty^{1/n} - C_\infty \tag{34}$$

and the corresponding horizontal Nusselt number is expressed as follows:

$$Nu_{\mathrm{h},\infty} = \overline{Nu_{\mathrm{h},\infty}} = 1 - A_n Ra^{2/n} C_\infty^{2/n} - B_n Ra^{1/n} C_\infty^{-1+1/n} \tag{35}$$

N	y_0	A_n	B_n
0.6	0.199	-0.485×10^{-7}	0.186×10^{-3}
1.0	0.211	-0.276×10^{-5}	0.139×10^{-2}
1.4	0.219	-0.160×10^{-4}	0.333×10^{-2}

Table III.
Dependence of y_0, A_n and B_n on n

Results and discussion

Numerical results for laminar natural convection flow and heat transfer of viscous power-law fluids are presented in the following subsections. The parameters a and Ra, were varied in wide ranges for shear-thinning ($n = 0.6$), Newtonian ($n = 1$) and shear-thickening ($n = 1.4$) fluids. On the basis of previous studies, conducted by Ng and Hartnett (1986), Mamou *et al.* (2001) and, more recently, by Inaba *et al.* (2003a, b), the solutions were found to be rather insensible to the Prandtl number variations, provided that this parameter is large enough as it is the case for the non-Newtonian fluids and also for a large category of fluids having a Newtonian behaviour. Therefore, Pr is not considered as an influencing parameter in this study. This finding is also confirmed by the present analytical solution which, in its range of validity, is independent of Pr. On the other hand, thermal boundary conditions corresponding to uniform imposed heating fluxes lead to flow characteristics independent of the aspect ratio, A, when this parameter is large enough. The approximate analytical solution, developed in the preceding section, on the basis of the parallel flow assumption, is thus valid asymptotically in the limit of a shallow cavity ($A \gg 1$). To determine the smallest value of A leading to results reasonably close to those of large aspect ratio approximation, various numerical tests were performed by progressively increasing this parameter from its lower value corresponding to a square cavity ($A = 1$). It is to mention that natural and anti-natural steady solutions were obtained both analytically and numerically. The corresponding natural/(anti-natural) flow is clockwise/(counter-clockwise) for $a > 0$ and counter-clockwise/(clockwise) for $a < 0$.

Let us note that the results, presented and discussed in this paper, can interest some manufacturing processes, involving non-Newtonian shear-thinning or shear-thickening fluids, where thermal buoyancy induced effects play a crucial role.

Validation of the approximate analytical solution

For $a = 0.1$, $A = 12$, $Ra = 4{,}000$ and different values of n, comparison between numerical (full and empty circles) and analytical (solid lines) results, shown in Figure 3, shows an excellent agreement in terms of vertical distributions of velocity and temperature at mid-length of the cavity. In addition, computed and calculated values of ψ_c, Nu_v and Nu_h, shown in Figures 4-6, respectively, for $n = 0.6$, 1.0 and 1.4, agree also well for a wide range of Ra and various values of a. Moreover, these results confirm that the value $A = 12$ satisfies the asymptotic limit of a shallow cavity for the present problem.

Effect of the flow behaviour index

A close inspection of the streamlines shown in Figure 2, shows that the unicellular flow structure, which is characterised by a parallel aspect in the central part of the enclosure, is not qualitatively affected by the rheological behaviour. However, important quantitative changes are observed in the corresponding values of the flow intensity, ψ_c, which decreases in absolute value from 10.676 to 1.391 (for natural flow) and from 10.464 to 1.025 (for anti-natural flow) when n passes from 0.6 to 1.4. This means that an increase of n slows down the fluid circulation within the cavity and such a tendency is well confirmed by the velocity profiles shown in Figure 3(a). The isotherms shown in Figure 2 are qualitatively more sensitive to the rheological

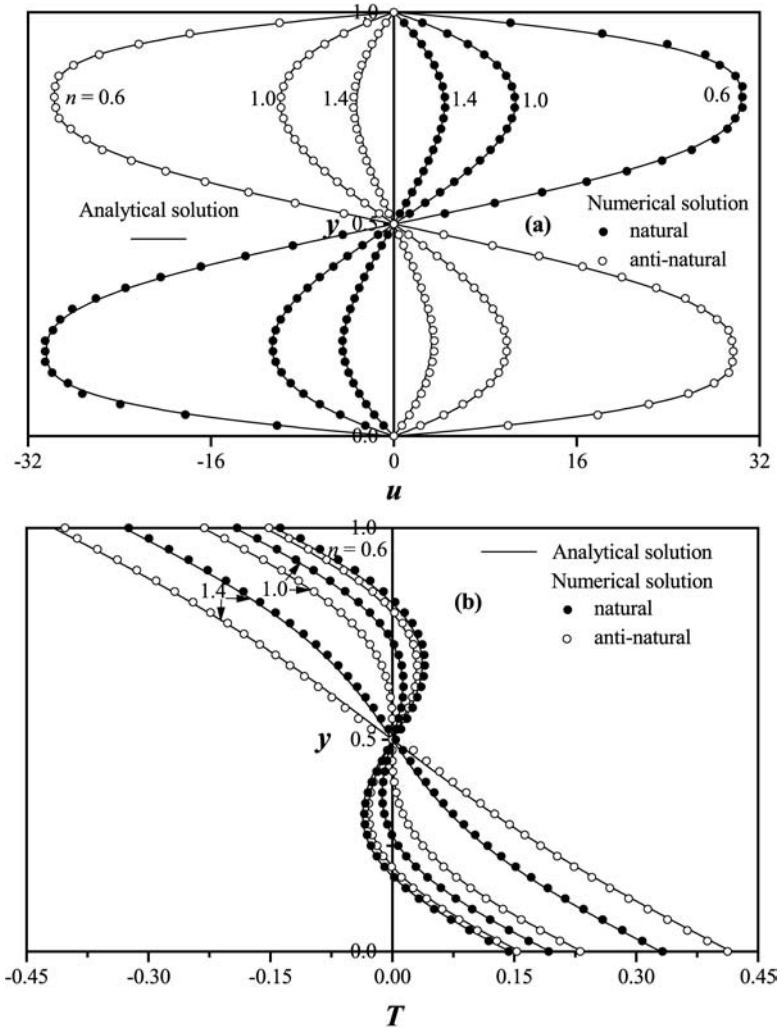

Figure 3.
Natural and anti-natural horizontal velocity (a) and temperature; (b) profiles along the vertical coordinate for $a = 0.1$, $A = 12$, $Ra = 4,000$ and different values of n

behaviour of the fluid than the streamlines. In fact, they show more important distortions for $n = 0.6$ since the most intense flow is generated by this value of n. The distortions tend to disappear for $n = 1.4$, and such behaviour is well corroborated by the temperature profiles shown in Figure 3(b). Accordingly, the mean Nusselt numbers, $(\overline{Nu}_v, \overline{Nu}_h)$, drop from (3.541, 0.839) to (1.515, 0.217) for the natural flow and from (3.211, 1.219) to (0.846, 0.347) for the anti-natural one when n is increased from 0.6 to 1.4. Such results confirm the reducing role of the dilatant behaviour with regard to the convection heat transfer and agree with similar observations reported in the past by Amari *et al.* (1994) while investigating natural convection in a horizontal rectangular porous layer saturated with non-Newtonian fluids.

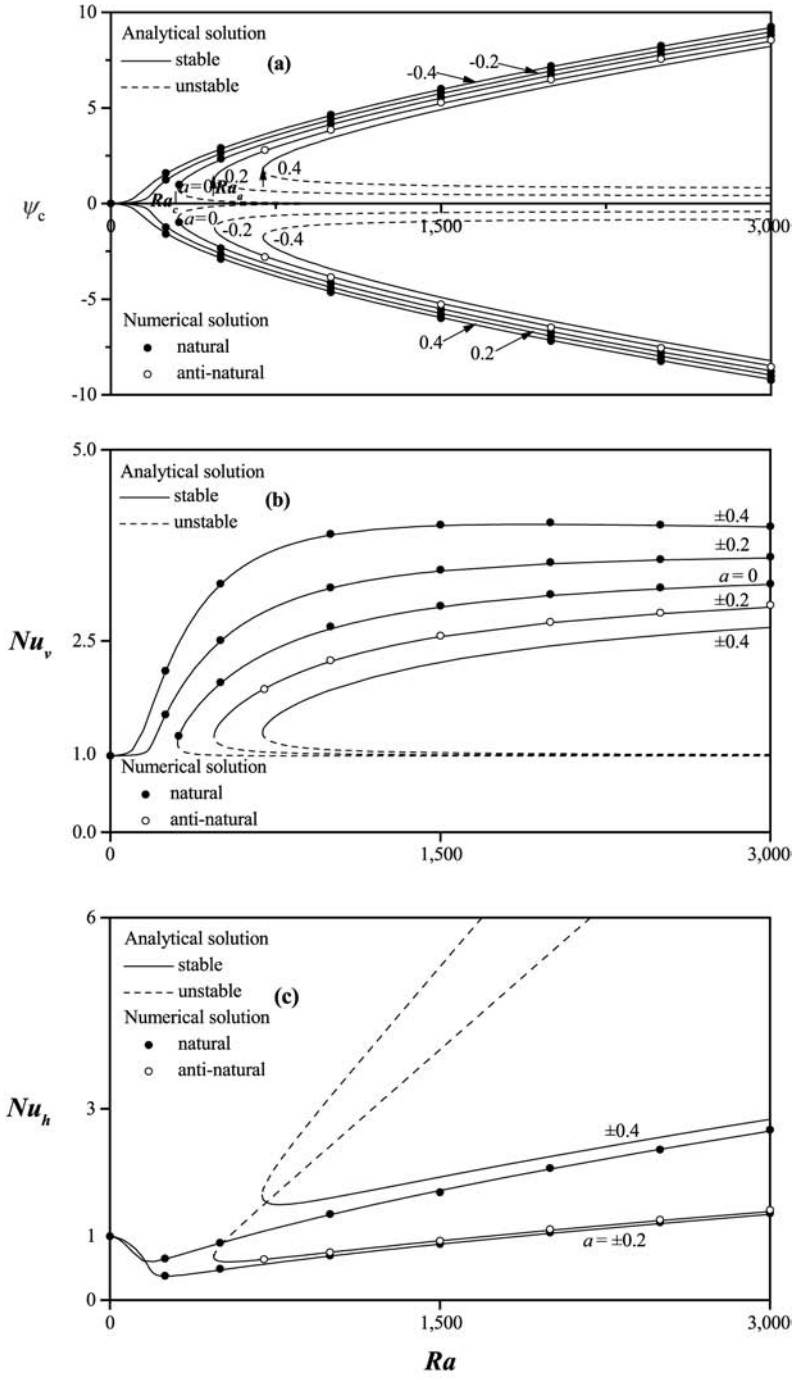

Figure 4.
(a) Flow intensity, ψ_c; (b) vertical Nusselt number, Nu_v and (c) horizontal Nusselt number, Nu_h, versus *Ra,* for various values of a, $A = 12$ and $n = 0.6$

Effect of the Rayleigh number

In Figures 4(a)-(c)-6(a)-(c) are shown the evolutions of the flow intensity, ψ_c(a), the vertical, Nu_v(b), and the horizontal, Nu_h(c), Nusselt numbers versus Ra, for $n = 0.6$ (Figures 4(a)-(c)), $n = 1.0$ (Figures 5(a)-(c)) and $n = 1.4$ (Figures 6(a)-(c)) and various values of a. For $a = 0$, the onset of motion occurs at $Ra = Ra_c$ and the rest state, characterised by $\psi_c = 0$, $Nu_v = 1$ and $Nu_h = 0$, becomes unstable. Hence, the stationary convection starts from the rest state at Ra_c and the unicellular corresponding flow is either clockwise or counter-clockwise rotating. Let us specify that Ra_c can be determined analytically for the Newtonian case, but for complex fluids, this parameter is estimated numerically since equation (30) presents a singular character when the constant axial temperature gradient C tends towards zero which is the case in pure conductive regime. In fact, for this regime, the power-law model is not valid; it does not consider the Newtonian behaviour of the fluid for the very low shear rates. For $a \neq 0$, three roots are theoretically possible when Ra is large enough. The curves with only one branch correspond to "natural" circulation (flow ascending at the level of the lateral heating surface) and the corresponding numerical values are represented by full circles, whereas the curves with two branches are related to "anti-natural" circulation (flow descending at the level of the lateral heating surface), starting beyond a threshold value of Ra, denoted Ra_a ($Ra_c > Ra_c$), which depends on a for a given value of n. For this type of flow, the portions of curves indicated by dashed lines were not accessible numerically, for all the explored values of a, n and Ra, and this, despite the numerous tests conducted with favourable initial conditions. In all previous studies using the parallel flow approximation (Sen *et al.* (1988), Kalla *et al.* (1999) and many other authors), it was not possible to confirm numerically the results of the unstable branch, and this, independently of the initial conditions used to initiate the numerical runs. The portions of curves with continuous lines corresponding to anti-natural flow were validated numerically (open circles) for $|a| < 0.4$ (with $a \neq 0$) and Ra varying in the ranges $304 < Ra \leq 10^4$ (for $n = 0.6$), $720 < Ra \leq 4.10^4$ (for $n = 1.0$) and $810 < Ra \leq 10^5$ (for $n = 1.4$).

The same figures show also different evolutions of the quantities ψ_c, Nu_v and Nu_h with Ra. In fact, for the natural flow $|\psi_c|$ and Nu_v are increasing functions of Ra whereas Nu_h does not follow the same evolution since it decreases from the unit to reach a minimum before increasing afterwards. For the anti-natural flow, the stable branch, of each curve, corresponds to an increase of ψ_c, Nu_v and Nu_h with Ra while a slight decrease/(increase) with this parameter is observed for ψ_c and Nu_v/(Nu_h) in the case of the unstable branch. Similar tendencies in the evolution of ψ_c and Nu_v, were reported by Kalla *et al.* (1999) for the case of a horizontal porous cavity saturated with a Newtonian fluid ($n = 1.0$) and subject to uniform heat fluxes on all sides.

These obtained results confirm the existence of multiple solutions for this kind of problem and the validity of the parallel flow hypothesis for a wide range of Ra. They also demonstrate clearly that Ra and n have opposite effects on fluid flow and heat transfer characteristics. In fact, for a given n, an increase of Ra enhances convection heat transfer whereas a decrease of n, for a given Ra, can induce a similar effect. However, the convection is found to be more sensitive to the change of Ra for fluids having pseudo-plastic behaviour ($0 < n < 1$) than for dilatant fluids ($n > 1$). This explains the choice of a reduced range of Ra in Figures 4-6 while varying n from 1.4 to 0.6 to allow a clear presentation of the curves corresponding to ψ_c, Nu_v and Nu_h.

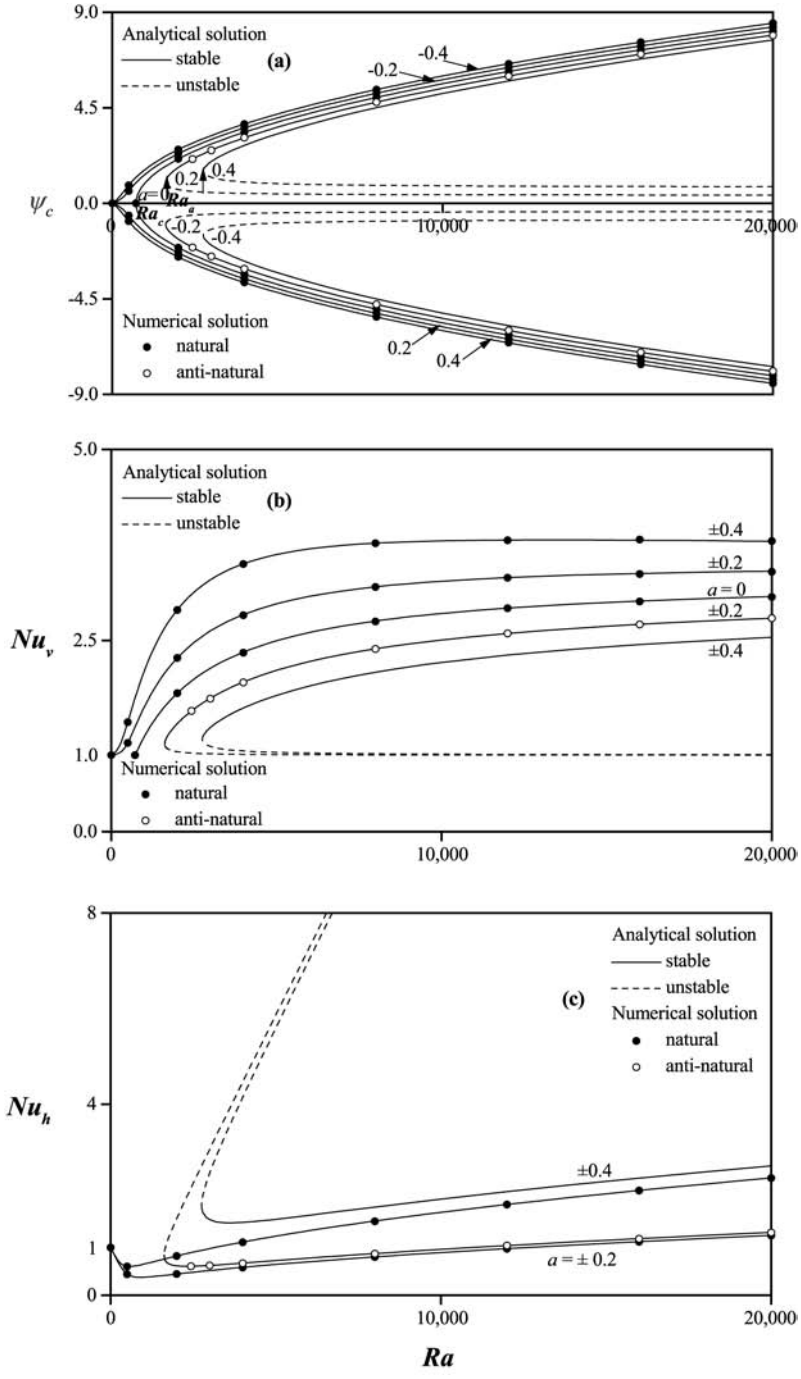

Figure 5.
(a) Flow intensity, ψ_c; (b) vertical Nusselt number, Nu_v and (c) horizontal Nusselt number, Nu_h, versus Ra, for various values of a, $A = 12$ and $n = 1.0$

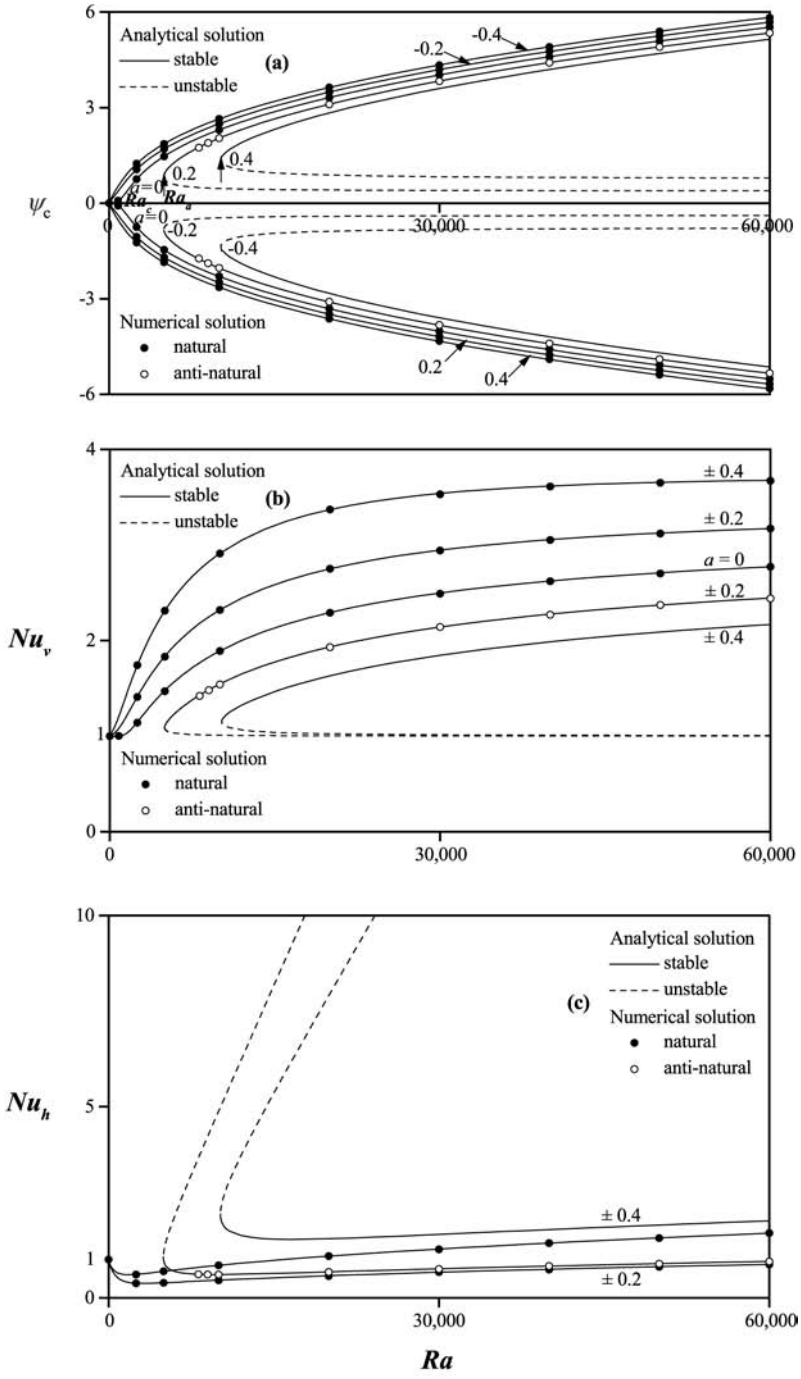

Figure 6.
(a) Flow intensity, ψ_c; (b) vertical Nusselt number, Nu_v and (c) horizontal Nusselt number, Nu_h, versus Ra, for various values of a, $A = 12$ and $n = 1.4$

The results obtained with the power-law model (which was used in the present study to characterise the non-Newtonian behaviour) are compared with those resulting from Ellis model (Ozoe and Churchill, 1972) in Figure 7. For the latter, the apparent viscosity varies with the generalised shear rate following the implicit relationship:

$$\frac{1}{\mu_a} = k_0 + k_1 \left[2 \left[\left(\frac{\partial u}{\partial x} \right)^2 + \left(\frac{\partial v}{\partial y} \right)^2 \right] + \left[\frac{\partial u}{\partial y} + \frac{\partial v}{\partial x} \right]^2 \right]^{m-1} \mu_a^{m-1} \tag{36}$$

A reasonable agreement between the results obtained with both models is seen in Figure 7 what makes evident the validity of the Ostwald-De Waele model at low convection. Equation (36), which takes into account the Newtonian behaviour at low shear rates, was solved for μ_a at each grid point and time by the Newton-Raphson method using the values of the velocity components at the previous time-step. Otherwise the procedure of calculation was the same as that previously described for the Ostwald-de Waele model. In the computational procedure used for the Ellis model, the following dimensionless coefficients, given in the paper of Ozoe and Churchill (1972) for 4 per cent CMC solution, were considered: $k_0 = 0.636$, $k_0 = 0.636$, $k_1 = 0.644$ and $m = 1.17$. The viscosity versus the shear-stress curve for the Ellis fluid is equivalent to that of an Ostwald-de Waele fluid with $n = 0.875$ and $k = 0.2065\,\text{Pa.s}^n$ over the range of shear-stress from 0.8 to 44 Pa. Note that the Ellis model, which is only used for shear-thinning fluids, involves three empirical constants and provides an implicit relationship between the rate of strain and the shear stress.

Effect of the side lateral heating intensity

To clarify the effect of the side heating intensity, a, on the thermal convection, both numerical and analytical results of ψ_c, Nu_v, and Nu_h are shown in Figures 8-10, respectively, for $n = 0.6, 1.0$and1.4 and various values of Ra. Recall that the change of the sign of a changes only the sign of ψ_c without affecting Nu_v and Nu_h. On the other hand, the variations of Nu_v with a present a discontinuity in the case of the "natural" solution, since Nu_v tends towards infinity when a approaches an asymptotic value a_∞ given by equation (34). This means that an inversion of the temperature sign occurs at the level of the horizontal boundaries. In addition, it is seen from the figures that the evolution of Nu_h with a, in the case of the "anti-natural" solution, presents different shapes according to the value of n. In fact, while passing from shear thickening behaviour ($n = 1.4$) to shear thinning one ($n = 0.6$), a spectacular evolution curiously similar to a flower blooming is observed. Moreover, it may be observed, from the same figures, that for a given (n, Ra) there is a critical value, $|a_a|$, of $a \neq 0$, which is a decreasing/(increasing) function of n/(Ra), for the existence of the anti-natural solution. These results confirm, also, the complexity in the behaviour change when the side heating intensity counts among the controlling parameters of the problem. Here again the numerical solution is seen to be in good agreement with the analytical parallel flow one.

For the evolutions of ψ_c and Nu_v with a, an analogous behaviour was observed in the past by Kalla *et al.* (1999) while studying buoyancy convection in a horizontal porous cavity saturated with a Newtonian fluid ($n = 1.0$) and submitted to uniform heat fluxes on all sides.

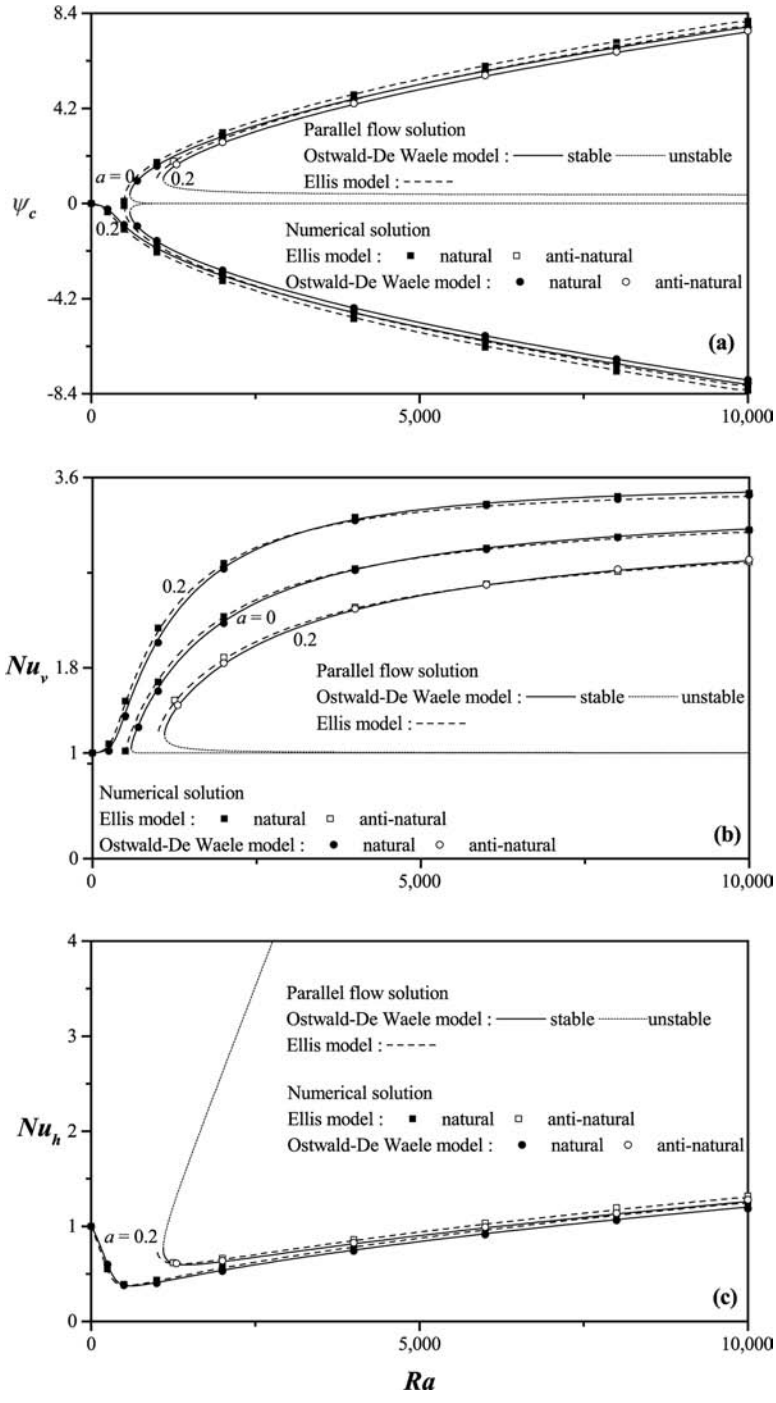

Figure 7.
(a) Flow intensity, ψ_c; (b) vertical Nusselt number, Nu_v and (c) horizontal Nusselt number, Nu_h, versus *Ra*, for $A = 12$ and two values of a. Comparison between results obtained with the Ostwald-De Waele ($n = 0.85$) and Ellis ($k_0 = 0.636$, $k_1 = 0.644$ and $m = 1.17$) models

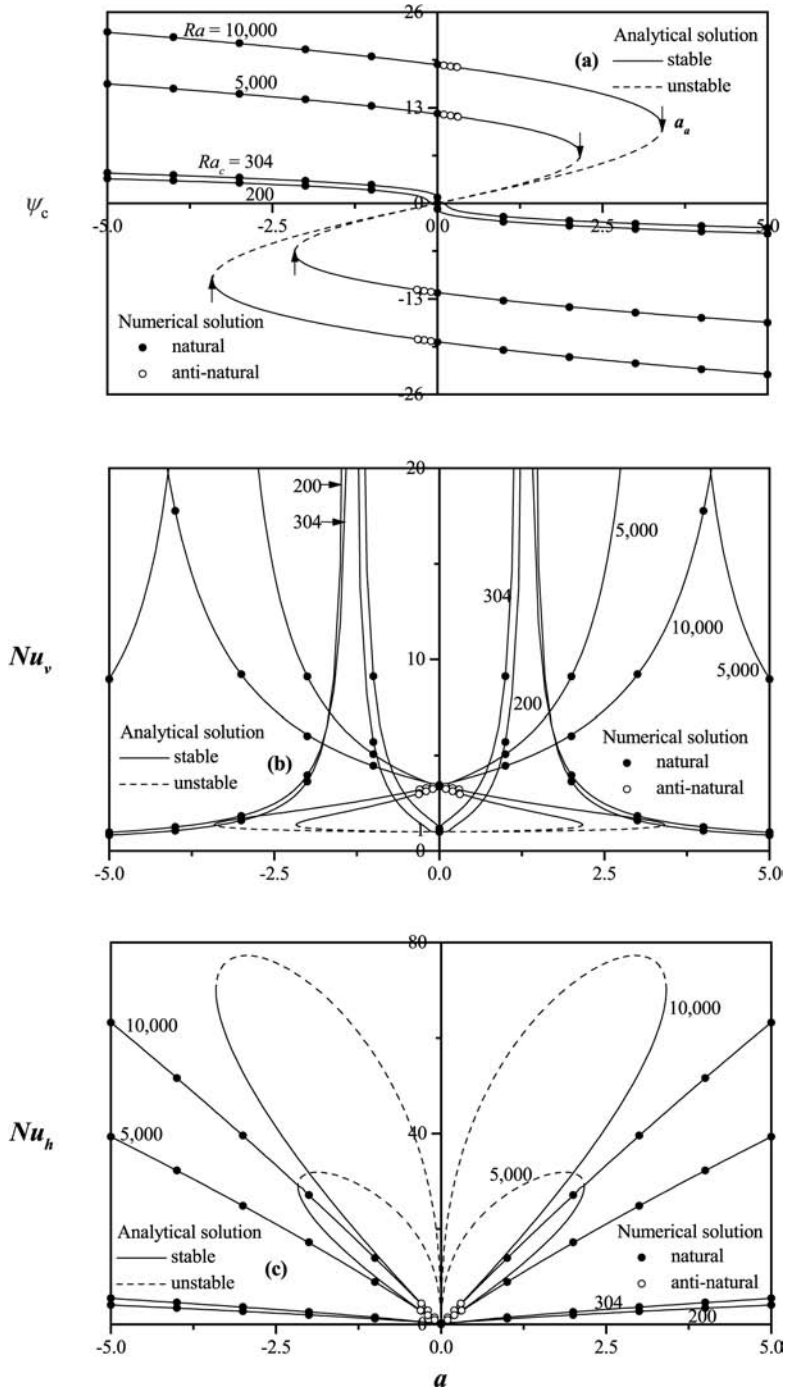

Figure 8.
(a) Flow intensity, ψ_c; (b) vertical Nusselt number, Nu_v and (c) horizontal Nusselt number, Nu_h, versus a, for $A = 12$, $n = 0.6$ and various values of Ra

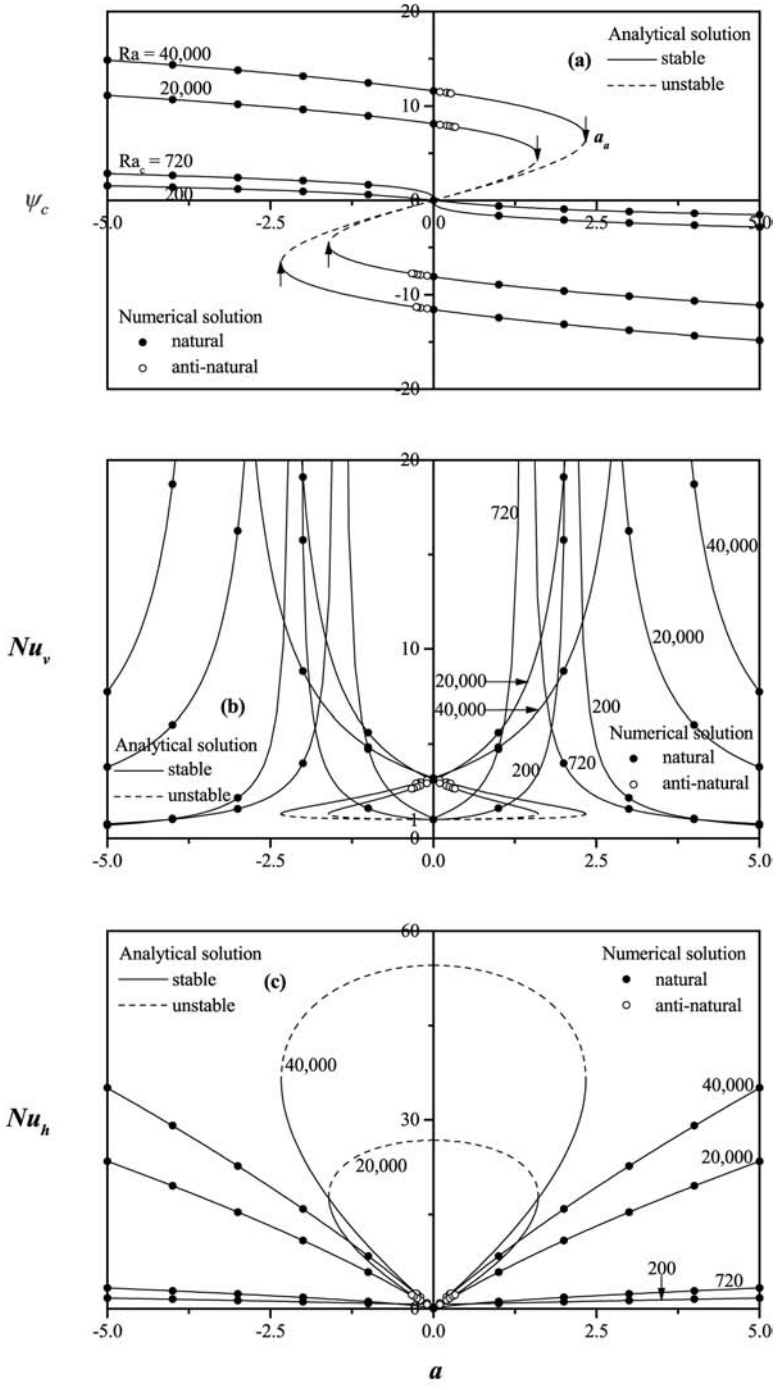

Figure 9.
(a) Flow intensity, ψ_c; (b) vertical Nusselt number, Nu_v, and (c) horizontal Nusselt number, Nu_h, versus a, for $A = 12$, $n = 1.0$ and various values of Ra

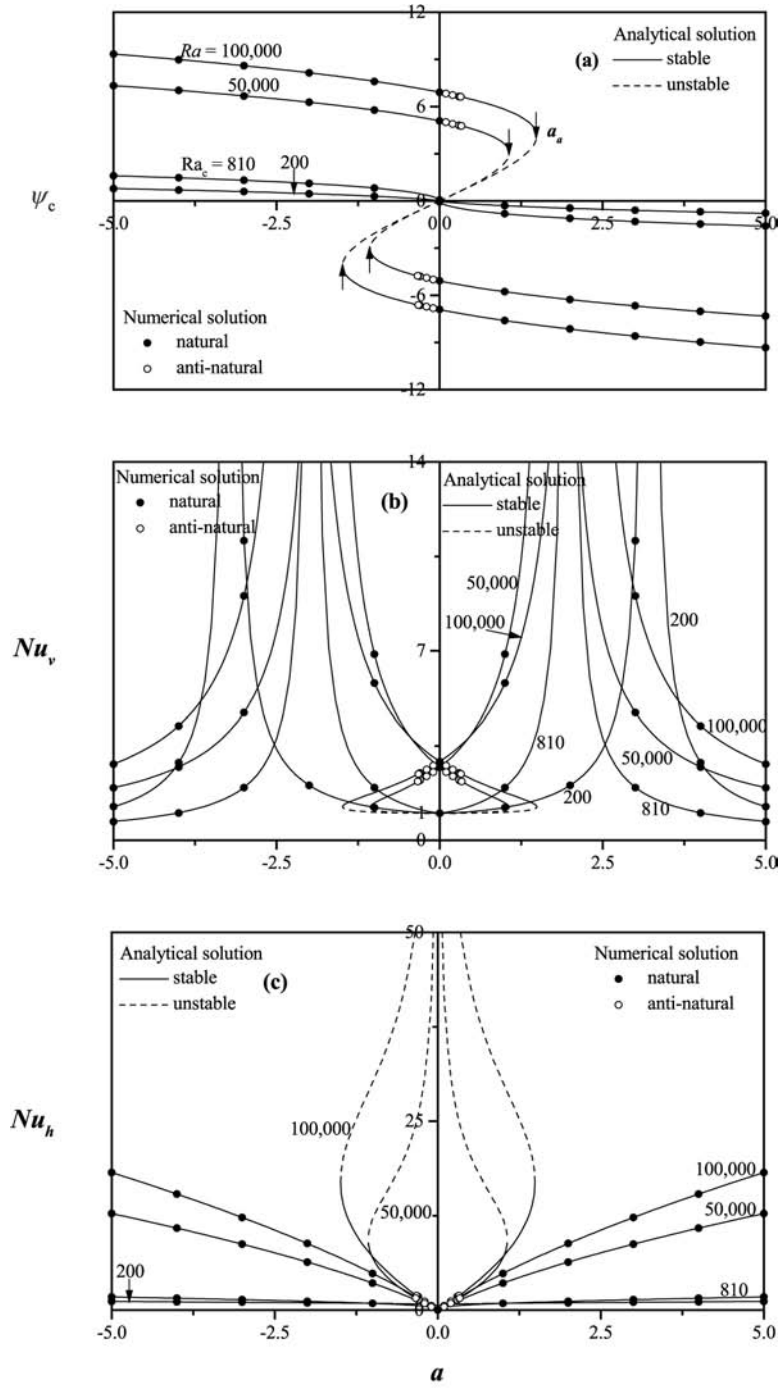

Figure 10.
(a) Flow intensity, ψ_c; (b) vertical Nusselt number, Nu_v, and (c) horizontal Nusselt number, Nu_h, versus a, for $A = 12$, $n = 1.4$ and various values of Ra

Conclusion

In this paper, the problem of steady natural convection, within a horizontal rectangular cavity filled with non-Newtonian power-law fluids and heated from all sides, was studied both numerically and analytically. The conjugate effect of the power-law index, n, the Rayleigh number, Ra, and the side heating intensity, a, on the flow intensity and heat transfer characteristics is investigated. The main results of the study are summarised in the following points:

- Under the conditions of imposed constant heat fluxes on all boundaries, the parallel flow structure is maintained in the core region of the enclosure provided that the aspect ratio of the cavity is large enough.
- For $a \neq 0$, the existence of two unicellular convective motions, namely "natural and anti-natural" flows, was proved when Ra exceeds a critical value and the value of a is chosen inside a specific range. Such a behaviour is not observed in the absence of lateral heating ($a = 0$). The two solutions engender different flow and heat transfer characteristics.
- The fluid flow and heat transfer are found to be rather sensitive to the non-Newtonian power-law behaviour. Compared to Newtonian fluids($n = 1$), a shear-thinning behaviour ($0 < n < 1$) enhances the fluid circulation and the convection heat transfer while the shear-thickening behaviour ($n > 1$) produces an opposite effect.
- The analytical results, based on the parallel flow assumption, are found to agree well in the core region with those obtained numerically by solving the full governing equations. There are however some portions in the anti-natural range of the analytical solution, named unstable, which were not validated numerically since their numerical obtaining was impossible despite the choose of favourable initial conditions.

References

Amari, B., Vasseur, P. and Bilgen, E. (1994), "Natural convection of non-Newtonian fluids in a horizontal porous layer", *Warmer-und Stoffübertragung*, Vol. 29, pp. 185-93.

Bejan, A. (1983), "The boundary layer regime in a porous layer with uniform heat flux from the side", *Int. J. Heat Mass Transfer*, Vol. 26, pp. 1339-46.

Bird, R.B., Armstrong, R.C. and Hassager, O. (1987), "Dynamics of polymeric liquids", *Fluid Mechanics*,Vol. 1, Wiley, New York, NY.

Cardon, X. (1989), "Etude expérimentale de la convection naturelle au sein d'une cavité rectangulaire, dans un fluide de type Ostwald-de-Waele à propriétés thermodépendantes", Thèse de Doctorat, Université de Nantes.

Gourdin, A. and Boumahrat, M. (1989), "Résolution des équations non linéaires, TEC& Doc-Lavoisier, Méthodes Numériques Appliquées", Paris, pp. 25-60.

Gray, D.D. and Giorgini, A. (1976), "The validity of the Boussinesq approximation for liquids and gases", *Int. J. Heat Mass Transfert*, Vol. 19, pp. 545-51.

Inaba, H., Daib, C. and Horibe, A. (2003a), "Numerical simulation of Rayleigh-Bénard convection in non-Newtonian phase-change-material slurries", *Int. J. Thermal Sciences*, Vol. 42, pp. 471-80.

Inaba, H., Daib, C. and Horibe, A. (2003b), "Natural convection heat transfer of micro-emulsion phase-change-material slurry in rectangular cavities heated from below and cooled from above", *Int. J. Heat and Mass Transfer*, Vol. 46, pp. 4427-38.

Jaluria, Y. (2003), "Thermal processing of materials: from basic research to engineering", *Journal of Heat Transfer*, Vol. 125, pp. 957-79.

Kalla, L., Mamou, M., Vasseur, P. and Robillard, L. (1999), "Multiple steady states for natural convection in a shallow porous cavity subject to uniform heat fluxes", *Int. Comm. Heat Mass Transfer*, Vol. 26 No. 6, pp. 761-70.

Mamou, M., Vasseur, P. and Hasnaoui, M. (2001), "On numerical stability analysis of double-diffusive convection in confined enclosures", *J. Fluid Mech.*, Vol. 433, pp. 209-50.

Ng, M.L. and Hartnett, J.P. (1986), "Natural convection in power-law fluids", *Int. Comm. Heat Mass Transfer*, Vol. 13, pp. 115-20.

Ohta, M., Ohta, M., Akiyoshi, M. and Obata, E. (2002), "A numerical study on natural convective heat transfer of pseudo-plastic fluids in a square cavity", *Num. Heat Transfer, Part A*, Vol. 41 No. 4, pp. 357-72.

Ozoe, H. and Churchill, S.W. (1972), "Hydrodynamic stability and natural convection in Ostwald-De Waele and Ellis fluids: the development of a numerical solution", *AIChE J.*, Vol. 18 No. 6, pp. 1196-207.

Prud'homme, M. and Bougherara, H. (2001), "Linear stability of free convection in a vertical cavity heated by uniform heat fluxes", *Int. Comm. Heat Mass Transfer*, Vol. 28 No. 6, pp. 743-50.

Prud'homme, M., Bougherara, H. and Bahloul, A. (2003a), "Convection in a vertical cavity submitted to crossed uniform heat fluxes", *Int. J. Heat Mass Transfer*, Vol. 46, pp. 3831-40.

Prud'homme, M., Hung Nguyen, T. and Bougherara, H. (2003b), "Stability of convection flow in a horizontal layer heated by uniform heat fluxes", *Int. Comm. Heat Mass Transfer*, Vol. 30 No. 2, pp. 163-72.

Roache, P.J. (1982), *Computational Fluid Dynamics*, Hermosa Publishers, Albuquerque, NM.

Sen, M., Vasseur, P. and Robillard, L. (1988), "Parallel flow convection in a tilted two-dimensional porous layer heated from all sides", *Phys. Fluids*, Vol. 31 No. 12, pp. 3480-7.

Sibony, M. and Mardon, J-CI (1982), "Approximation, interpolation, dérivation et intégration numérique", Hermann, Editeurs des Sciences et des Arts, Analyse Numérique II, Approximation et Equations Différentielles, Paris, pp. 89-118.

Tien, C., Tsuei, H.S. and Sun, Z.S. (1969), "Thermal instability of a horizontal layer of non-Newtonian fluid heated from below", *Int. J. Heat Mass Transfer, Shorter Communications*, Vol. 12, pp. 1173-8.

Turki, S. (1990), "Contribution à l'étude numérique des transferts par convection naturelle et par convection mixte dans les fluides non-Newtoniens confinés", Thèse de Doctorat, CNAM, Paris.